Identification of alkaline amendment sources (slash and burn versus marling) for cereal crops grown in the North of France: a multiple isotope approach (87Sr/86Sr, δ44/40Ca, δ88/86Sr)

A.-D. Schmitt, T. Hoang Trinh, S. Gangloff, V. Matterne, F. Spicher, B. Brasseur

Journal Pre-proof

Identification of alkaline amendment sources (slash and burn versus marling) for cereal crops grown in the North of France: a multiple isotope approach ($^{87}Sr/^{86}Sr$, $\delta^{44/40}Ca$, $\delta^{88/86}Sr$)

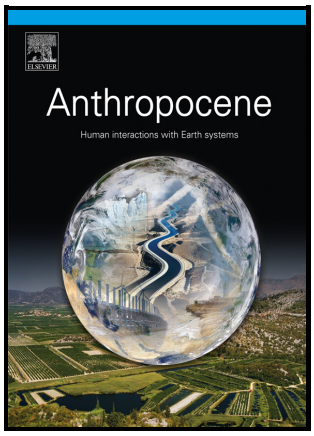

A.-D. Schmitt, T. Hoang Trinh, S. Gangloff, V. Matterne, F. Spicher, B. Brasseur

PII: S2213-3054(23)00023-1

DOI: https://doi.org/10.1016/j.ancene.2023.100390

Reference: ANCENE100390

To appear in: *Anthropocene*

Received date: 7 September 2022
Revised date: 21 May 2023
Accepted date: 10 June 2023

Please cite this article as: A.-D. Schmitt, T. Hoang Trinh, S. Gangloff, V. Matterne, F. Spicher and B. Brasseur, Identification of alkaline amendment sources (slash and burn versus marling) for cereal crops grown in the North of France: a multiple isotope approach ($^{87}Sr/^{86}Sr$, $\delta^{44/40}Ca$, $\delta^{88/86}Sr$), *Anthropocene,* (2023) doi:https://doi.org/10.1016/j.ancene.2023.100390

Identification of alkaline amendment sources (slash and burn versus marling) for cereal crops grown in the North of France: a multiple isotope approach ($^{87}Sr/^{86}Sr$, $\delta^{44/40}Ca$, $\delta^{88/86}Sr$)

Schmitt A.-D.[1*], Hoang Trinh T.[1], Gangloff S.[1], Matterne V.[2], Spicher F.[3], Brasseur B.[3*]

[1]Université de Strasbourg, CNRS, ITES, UMR 7063, 67084, Strasbourg, France

[2]CNRS/MNHN, UMR 7209 AASPE – Archeozoologie et Archéobotanique : Sociétés, Pratiques et Environnements, 55 rue Buffon, CP56, 75005 Paris, France

[3]UMR7058 EDYSAN, Université de Picardie Jules Verne, Pôle Santé, 80021, Amiens, France

[*]Corresponding authors:

B. Brasseur (boris.brasseur@u-picardie.fr) & A.-D. Schmitt (adschmitt@unistra.fr)

Acknowledgements

This project was financially supported by the French CNRS-INSU program « EC2CO- HYBIGE », as well as through an M2 internship by the French"Fondation pour la recherche surla biodiversité" (FRB). Elemental and isotopic analyses were performed at the Pacite platform of the University of Strasbourg at ITES (Strasbourg – France). We are very grateful to Jean and Véronique Hennequart who agreed to make their cleared plot available and actively contributed to the monitoring of the experimental plot. We also thank Colin Fourtet and René Boutin for measuring major and trace element concentrations and Eric Pelt for his help with the Triton. Anne-Désirée Schmitt wishes to thank François Chabaux for many constructive discussions. The manuscript benefitted from constructive reviews by four anonymous reviewers. The editorial team and the editor are thanked for their handling of the manuscript.

Abstract

Early farmers used at least two types of agrarian amendments that could raise pH and base saturation levels to allow the cultivation of cereals: marling and plant ash. Ash can be input in many different ways: felling and burning in place, transferring plant material from wastelands and spreading the ash, charring sod or peat blocks, burning stubble after harvest. Marling includes all the practices of amending limestone, from marl to chalky limestone composed of 99% $CaCO_3$.

In order to understand the evolution of these agricultural practices, it is important to identify which of the two techniques was used to amend cereal crops in the past. In order to test the

potential of $\delta^{44/40}$Ca-$\delta^{88/86}$Sr-^{87}Sr/^{86}Sr multiple isotope approach for archaeological samples, we first applied the technique to currently grown crops, amended either with marl or with ash from freshly-cut and burned trees. We found that this approach makes it possible to discriminate cereal grains amended either by marling (less radiogenic Sr) or with tree ash (more radiogenic Sr). We also identified a positive correlation between stable Ca and Sr isotope values, suggesting that the Ca and Sr came from similar sources and had undergone similar mass-dependent isotopic fractionation mechanisms. Consequently, we later on mainly focused on stable and radiogenic Sr isotopes. Stable Sr isotope fractionation was also observed between different locations, different organs of a given cereal species and between different cereal types, but also within the same cereal species or the number of grains studied for a given locality, pointing to biological fractionation combined with source variation.

Keyword

Cereals, isotopes, soils, ash spreading, marling

1. Introduction

pH is a fertility indicator in forest and agricultural soils. In humid climates, the leaching of anions and cations naturally leads to progressive soil acidification (Slessarev et al., 2016) over time and depth (Brasseur et al., 2018). Under a pH of 5, this depletion of the cationic charge (base-cation saturation ratio) is associated with the increasing bioavailability of Al^{3+} and H^{+} (Ritchie, 1989), a process responsible for the phenomenon of aluminium toxicity in plants (Scott and Fisher, 1989). Combined with the scarcity of nutrient cations, adverse effects on the metabolism of non-adapted plants will occur.

Acidophilic plants in oceanic temperate forests are able to withstand this phenomenon of soil acidification and maintain their metabolism at pH_{water} levels below 5. However, cultivated

wheat, derived from cultivars naturally present on alkaline soils in the Near East (Snir et al., 2015), have never adapted to such conditions and still suffer from aluminium toxicity (Arunakumara et al., 2013). As a result, early farmers in humid regions had to invent agrarian practices that could raise the pH and base saturation levels to adapt the soil to the requirements of these cereals. These practices have evolved over time and some, like marling and liming, are still used by farmers today (Läuchli and Grattan, 2017; Matthew, 1993).

The most common materials used for marling are the various limestones and their derivatives, such as lime (Goulding, 2016). However, in the absence of these materials, farmers may also use sandy deposits of calcareous seaweed (Clout and Phillips, 1972) or alkaline plant ash (Juo and Manu, 1996) generated during slash and burn practices. Burning provides nutrients via the ashes of the burned forest plots (Ehrmann et al., 2014). This may be one of the oldest techniques used (Rösch et al., 2017). However, spreading ash on cropland is not very sustainable, as the nutrients applied to the soil decrease very rapidly after a few years of cultivation, through leaching, erosion, runoff or direct absorption by the crops themselves (e.g. Juo and Manu, 1996 ; Palm et al., 1996 ; Fachin et al., 2021).

Marling, a very common practice in North-Western Europe, consists of spreading crushed rocks rich in carbonates such as chalk, marl and dolomite on agricultural soils. It has long-term effects on the soil and helps to improve soil structure through the formation of aggregates that can trap nutrients. This also promotes soil cohesion and gives the soil a more aerated texture (Goulding 2016; Goulding and Annis, 1998; Goulding et al., 1989).

In order to understand historical changes in agricultural practices, it is interesting to identify the use of one technique or the other to amend cereal crops over time, since the Neolithic colonization of temperate Europe (e.g. Rösch et al., 2017). Marling has had a lasting impact on the alkalinization of the soil. The practice is likely to have considerably changed the natural chemical evolutionary trajectory of the soils supporting the ecosystems in north-western Europe and its impact needs to be better measured. Marling also contributes to recharging the reserve

of basic cations, in particular of calcium (Ca^{2+}), an essential nutrient in plant metabolism (Marschner, 1995). The presence of sufficient quantities of Ca in the soil is essential for root development and to slow down the deficit in nutritive cations (Goulding and Annis, 1998). However, Ca levels are often very low in acid soils, thus limiting plant growth.

Because of the physicochemical similarities between strontium and calcium, the $^{87}Sr/^{86}Sr$ isotopes have been proposed as a source tracer for Ca since ^{87}Sr is radiogenic (e.g. Åberg et al., 1990 ; Clow et al., 1997 ; Capo et al., 1998 ; Probst et al., 2000 ; Poszwa et al., 2004 ; Bullen and Bailey, 2005 ; Drouet et al., 2005a ; Poszwa et al., 2009 ; Bagard et al., 2013). Drouet et al. (2005a ; 2005b) used the Ca/Sr elemental ratio and the $^{87}Sr/^{86}Sr$ isotope ratio to trace changes in Ca fluxes in a forest ecosystem in Belgium, as well as the pedological impacts 30 years after the application of a limestone amendment. Sr isotope ratio ($^{87}Sr/^{86}Sr$) has also been used to identify the Sr source of archaeological cereal seeds (e.g. Heier et al., 2009 ; Benson, 2012 ; Styring et al., 2019 ; Larsson et al., 2020).

In addition, during the last two decades, the stable isotopes of Ca ($\delta^{44/40}Ca$) and Sr ($\delta^{88/86}Sr$) have shown their potential to trace weathering mechanisms, the biological cycling of these elements and secondary mineral precipitation in soils (e.g. Schmitt et al., 2013 ; Shalev et al., 2013 ; Wei et al., 2013 ; Andrews et al., 2016 ; Bullen and Chadwick, 2016 ; Hajj et al., 2017 ; Schmitt et al., 2017 ; Brazier et al., 2019 ; 2020a ; Guibourdenche et al., 2020 ; Oeser and von Blanckenburg, 2020 ; Bouchez et al., 2021).

Our objective in the present study was to test the potential of $\delta^{44/40}Ca$-$\delta^{88/86}Sr$-$^{87}Sr/^{86}Sr$ multiple isotope approach on samples of present-day cereals grown on soils where two different Ca and Sr sources, wood ash and limestone, had been applied. To this end, different cereals (hulled barley, bread wheat, emmer, spelt, einkorn) were grown in North France in a freshly (2017) deforested plot on loessic luvisols. The plot was amended with tree ash from the spruce and oak trees previously growing on the site. The cereals' isotopic signatures were then compared to

those of the same cereals sown in long-deforested fields (since 1965 or for several centuries), also on loessic luvisols, which had been amended with chalk.

2. Materials and methods

2.1 Study site and sampling protocol

All field work, including the field cereal-growing experiments and sample collecting, was performed by the CNRS Research Unit EDYSAN (Amiens, France). Different cereal species were grown in 2018/2019 and 2019/2020 on haplic luvisols (WRB, 2015) in the Hauts-de-France region in northern France. The soils developed on decarbonated loess silt over 2 m thick. The underlying loess is still carbonated and rests on a bedrock of Upper Cretaceous chalk (Celet et al., 1979). The carbonated loess dates to the Late Pleniglacial period (Weichselian) (Haeserts, 1984; Antoine et al., 2001; 2016). Originally this loess contained about 10% Ca carbonate, 15% clay minerals (smectites, micas, kaolinite and interbedded minerals); the remainder of the sediment was mostly quartz with traces of feldspar, chlorite and amphibole (van Ranst et al., 1982).

The experimental plot (EP) was located in the Bois d'Arrouaise (Oisy, France) in Aisne county (Fig 1 a, b and c). The Bois d'Arrouaise is an old forest, more than 2000 years in age, mentioned in the archives of the 10th and 12th centuries (Gosse, 1786). This woodland was still vast at the beginning of the 19th century (7.7 km²), but then it underwent two major clearing episodes: in the second half of the 19th century (reduced to 0.58 km²), and then at the end of the 1960s (reduced to 0.39 km²). Although the deforested land was mainly used for livestock farming at the end of the 19th century, it was gradually converted to agricultural land in the early 1990s.

The tree species cut on the EP were common spruce (*Picea abies*), pedunculate oak (*Quercus robur*) and a few beech (*Fagus sylvatica*). One parcel was deforested in 2017. Cereal seeds were then sown there. The EP soil was amended with 40 kg/m² of ash (and a few pieces of

charcoal) from spruce and oak trees cut on site (see effect on pH in the supplementary material section). The cereals were sown in November 2018 and March 2019, and harvested towards the end of July/beginning of August, in 2019 and 2020 respectively.

Other cereals grown on four different agricultural plots that had been amended with chalk from the Paris Basin, France were analysed additionally to the EP plot: one conventionally grown (CONV) plot located at the edge of the Bois d'Arrouaise, 100 m from the experimental plot (Fig. 1a and b) and three organically grown plots, two of which were located in Hiermont (HIER1 and HIER2; Fig. 1d) and one in Gouzeaucourt (GOUZ, Fig. 1a). The cereals on these plots were harvested in summer 2019 and analysed (Table 1).

There are three types of samples from the five experimental plots: soils, amendments and cereals. Soils from the EP plot were collected at 4 different depths: 0-10 cm, 20-30 cm, 45-55 cm and 95-105 cm, whereas soils from the CONV, HIER1, HIER2, and GOUZ agricultural plots were collected only at the surface (0-10 cm). A loess sample was collected at depth (350-450 cm) at Havrincourt Wood (near Gouzeaucourt). The amendments used to fertilize these soils (wood ash in the case of EP and crushed chalk for the four other plots) were collected at each location. Atmospheric inputs (wet deposits and dust) were collected in a polypropylene water tank at the Bois d'Arrouaise near EP from March to November, 2020. For the EP plot, the cereals harvested were: hulled barley (*Hordeum vulgare* subsp. *vulgare*), einkorn (*Triticum monococcum* subsp *monococcum*), bread wheat (*Triticum aestivum* subsp *aestivum*), spelt wheat (*Triticum aestivum* subsp. *spelta*) and emmer (*Triticum turgidum* subsp. *dicoccon*). On the HIER2 plot, we harvested hulled barley, and on HIER1, rivet wheat (*Triticum turgidum* subsp. *turgidum*) and bread wheat. On the GOUZ and CONV plots, we collected bread wheat. The caryopses were analysed for all these cereals. In addition, other organs were analysed for some of the samples: straw for EP (hulled barley, bread wheat and emmer) and HIER2 (hulled barley), awns for EP (hulled barley and emmer) and HIER2 (hulled barley), and leaves for CONV (bread wheat) and EP (emmer).

2.2 Preparation, leaching, and digestion of the samples

All the sample preparations were performed at the Institut Terre et Environnement de Strasbourg (ITES, France). For the cereal grain analyses, 10 caryopses were collected for each type of cereal. In order to test for within-sample variability, we analysed ten caryopses grouped in a single batch and three caryopses grouped in another batch from the same hulled barley ear (OR1) and compared them to ten caryopses grouped in a single batch from another hulled barley ear (OR2) from the EP plot. We also analysed batches of 10, 3 and 1 caryopses from a same hulled barley ear (ORb) which we compared to 10 caryopses from another ear (ORa) from HIER2.

The cereal organs were charred at 450°C in a muffle furnace in Pyrex™ beakers previously rinsed with Millipore© ultrapure water and distilled HCl (90/10). To validate the carbonisation protocol, and to exclude any bias related to the use of this technique, a certified reference material (NIST SRM 1515, apple leaves) was also charred following the same protocol as for the cereal organs.

The soil samples and the loess sample were ground and sieved to 100 µm with a RS 100 vibratory disc mill (Retsch®) containing an agate grinding bowl (Retsch®). The chalk samples were manually ground in an agate mortar.

After the grinding procedure, approximately 2 g of each soil sample and 250 mg of each of the loess and chalk samples were collected for leaching. They were mixed with 10 mL of 0.5 N HCl and stirred at 40 rpm for 10 min on an SB3 Stuart™ rotator. The mixtures were then centrifuged at 4000 rpm for 10 min in a Thermo Jouan B4-I™ multifunction centrifuge and the supernatants were recovered and filtered at 0.22 µm. The same procedure was applied three times, then repeated again twice with Millipore© ultrapure water to recover all the carbonate and exchangeable fractions. These aliquots will be called leachates in the following. According to Abali et al. (2011) and Yan et al. (2016), this protocol is an acceptable compromise between

dolomite leaching and the non-digestion of silicate phases. In the absence of targeted soil water sampling (such as by porous candles), we will adopt the leachate as the most suitable proxy for the Ca and Sr composition that can be easily taken up by plants.

Between 100 and 250 mg of soil, loess and chalk residues (i.e., the minerals undigested during leaching), wood ash samples and plant organs were dissolved in successive acid baths (HF-HNO_3, $HClO_4$ and HCl-H_3BO_3) to achieve complete dissolution of the samples. The samples were then evaporated to dryness, dissolved in 10 mL of 0.5 N HNO_3, and stored for chemical and isotopic analyses (Pelt et al., 2013 ; Brazier et al., 2020a ; 2020b).

The total Ca and Sr from blank samples for this digestion procedure were less than 50 and 2 ng, respectively. This represents a negligible average contribution of maximum 0.009% and 0.063% to the Ca and the Sr of the samples, respectively.

The liquid sample of atmospheric deposits was filtered through 0.22 µm cellulose acetate membrane filters in the laboratory and acidified with distilled HNO_3 to a pH ~ 1 for the chemical and isotopic analysis. Then it was digested with distilled HNO_3 and 30% Merck® suprapure H_2O_2, evaporated to dryness, dissolved in 10 mL of 2% HNO_3, and stored in a refrigerator.

2.3 Analytical procedures

Elemental and isotopic analyses were performed at the Cortecs-Pacite platform of the University of Strasbourg at ITES (Strasbourg, France). Elemental measurements were performed on an ICP-AES (ThermoScientific iCAP 6000 series™) with an uncertainty comprised between 3 and 10% depending on the analysed element.

For the $\delta^{44/40}Ca$ analyses, 0.14 µmol of Ca from each sample was mixed with 0.01 µmol of Ca from a ^{42}Ca-^{43}Ca double spike ($^{42}Ca/^{43}Ca$ spike ratio of ~5) and dried at 70 °C on a hot plate. The mixtures were then dissolved in 2 N HNO_3 and chemical separations were performed on a DGA normal resin (TODGA, Triskem™) following Brazier et al.'s (2019) procedure. Eluted

Ca (~100% recovery) was dried a first time at 70 °C and converted into nitric form with 7 N HNO_3 before a second drying at 70 °C on a hot plate.

Concerning the $\delta^{88/86}Sr$ measurements, 4.62 nmol of Sr from each sample was mixed with 1.08 nmol of Sr from a ^{84}Sr-^{87}Sr double spike, while 5.70 nmol of Sr from each sample, without a double spike, was taken for the $^{87}Sr/^{86}Sr$ measurements. After the first step of drying at 70 °C, all the mixtures and samples were dissolved in 4N HNO_3, then Sr was chemically separated with a TODGA resin (Triskem™), according to Brazier et al.'s (2020b) elution procedure, for ~100% recovery. After Sr elution, all the samples were dried at 70 °C on a hot plate. The total Ca and Sr in the blanks for the chemical separation procedure represented less than 0.6 % and 0.04 %, respectively, and were considered to be negligible for the rest of this study.

The dried residues obtained after each chemical separation were dissolved in 1 to 3 µL of 1 N HNO_3 and deposited on: (1) single, previously outgassed and oxidized tantalum filaments (99.995% purity) (in a primary vacuum pump) for the $\delta^{44/40}Ca$ measurements; and (2) single, previously outgassed rhenium filaments (99.98 % purity) with a Ta_2O_5 activator for the $\delta^{88/86}Sr$ and $^{87}Sr/^{86}Sr$ measurements.

All the isotopic measurements were performed on a Thermo Scientific Triton™ TIMS in static and multi-dynamic mode for Sr and Ca measurements, respectively (for details of measurement procedure for Ca and Sr isotopes, see Schmitt et al., 2013 and Brazier et al., 2020b). $\delta^{44/40}Ca$ and $\delta^{88/86}Sr$ were expressed in permil ratios relative to NIST SRM915a and NIST SRM987, respectively:

$$\delta^{44/40}Ca = \left(\frac{(^{44}Ca/^{40}Ca)_{sample}}{(^{44}Ca/^{40}Ca)_{SRM915a}} - 1 \right) \times 1000 \quad (1)$$

$$\delta^{88/86}Sr = \left(\frac{(^{88}Sr/^{86}Sr)_{sample}}{(^{88}Sr/^{86}Sr)_{SRM987}} - 1 \right) \times 1000 \quad (2)$$

The average internal repeatability of the SRM 987 standard over the long term was 0.71025 ± 0.00003 (2SD, N=133) and 0.001 ± 0.021 ‰ (2SD, N=26), for $^{87}Sr/^{86}Sr$ and $\delta^{88/86}Sr$, respectively. That of the SRM 915a standard was 0.00 ± 0.07 ‰ (2SD, N=63), for $\delta^{44/40}Ca$. These values agree with the literature (Brazier et al., 2020a). Based on sample replicates, the external uncertainty is ± 0.00001 (2SD, N=8) and ± 0.023 ‰ (2SD, N=12) for $^{87}Sr/^{86}Sr$ and $\delta^{88/86}Sr$, respectively. To avoid drifts in $\delta^{44/40}Ca$ and $\delta^{88/86}Sr$ between different measurement sessions, the ^{84}Sr-^{87}Sr and ^{42}Ca-^{43}Ca double tracers were calibrated in each measurement session by measuring three mixtures of SRM 987 and SRM 915a standards, respectively, and applying a corresponding double tracer according to the protocol published by Lehn and Jacobson (2015). The accuracy of the respective Sr and Ca stable isotope measurements was guaranteed by measuring an IAPSO seawater standard (0.389 ± 0.028, 2SD, N=10) for stable Sr measurement and an in-house Atlantic seawater standard (0.89 ± 0.11, 2SD, N=26) for stable Ca measurement that agree with data in the literature (Hippler et al., 2003; Heuser et al., 2016; Brazier et al., 2020a). Based on these measurements, the external reproducibility of the Sr and Ca stable isotope measurements were 0.028 ‰ and 0.11 ‰, respectively.

2.4 Mixing calculations

The proportion X(Sr) of A in a mixture (M) between two sources A and B can be determined as follows (e.g. Capo et al., 1998; Drouet et al., 2005a):

$$X(Sr)_A = \frac{(^{87}Sr/^{86}Sr)_M - (^{87}Sr/^{86}Sr)_B}{(^{87}Sr/^{86}Sr)_A - (^{87}Sr/^{86}Sr)_B} \quad (3)$$

3. Results

All the elemental and isotopic values measured on loess, soil, chalk, ash, atmospheric deposits and cereal organs carried out during this work are presented in Table 2. The isotopic measurements of the international apple leaves NIST SRM 1515 standard, whether calcined or

not (Fig. 2), agree with the literature for both $^{87}Sr/^{86}Sr$ (0.71398 ± 0.00005, N=3) and $\delta^{88/86}Sr$ (0.244 ± 0.034, N=3) (Liu et al., 2016 ; Schuessler et al., 2018 ; Oeser and von Blankenburg, 2020 ; Uhlig et al., 2020 ; van Hamm-Meert et al., 2020). This indicates that calcination does not cause analytical bias and the data obtained with this technique can be compared with the literature.

Ca isotope variability was highest between the emmer caryopses from EP (-1.44 ‰) and the chalk leachate from HIER1 (0.62 ‰), resulting in a total fractionation amplitude of 2.06 ‰ (Fig. 3a). Within grains, the variability was more limited (1.22 ‰). It can be noted that there was variability between caryopses of the same cereal species grown in different fields. For example, for wheat, $\delta^{44/40}Ca$ was -1.04 ‰ at EP and -0.22 ‰ at HIER1 while hulled barley was -1.09 ‰ at EP and -0.82 ‰ at HIER2.

Within plant organs, stable Sr isotope variability was highest between the caryopse (-0.376 ‰) and the awn (0.595 ‰), i.e. a total amplitude of 0.971 ‰ (Fig. 3b). Within an organ type, the fractionation amplitude was also variable: 0.275 ‰ for caryopses (N=14), 0.228 ‰ for straw (N=4), 0.623 ‰ (N=3) for awns, 0.678 ‰ (N=2) for leaves and 0.204 ‰ (N=2) for glumes. $\delta^{88/86}Sr$ had the lowest isotopic signatures for caryopses (-0.259 ± 0.044 ‰, N=14, 2SE), followed by straw (-0.133 ± 0.109 ‰, N=4, 2SE), then glumes (-0.016 ± 0.204 ‰, N=2, 2SE), then leaves (0.171 ± 0.678 ‰, N=2, 2SE), and then finally, awns (0.180 ± 0.415 ‰, N=3, 2SE). The amplitude was lower in the other (non-cereal) samples analysed (0.235 ‰, N=21).

The Sr isotope ratio $^{87}Sr/^{86}Sr$ varied between 0.70739 (leached chalk) and 0.73423 (EP leached soil) (Fig. 3c). All the soil and chalk residues and EP leached soils tended towards the most radiogenic values, whereas all the leachates, atmospheric deposits and cereal organs tended towards the less radiogenic values. Loess residue and ash showed intermediate values.

If we look at the variability within hulled barley caryopses for EP, we notice that the radiogenic Sr compositions for OR1 are similar, within the analytical uncertainties (0.71199 and 0.71196) for ten and three caryopses, but different from OR2 (0.71211) (Table 2). Similarly, the $\delta^{88/86}Sr$

isotope compositions were different between ten caryopses of OR2 (-0.250 ‰) and three caryopses of OR1 (-0.329 ‰). Similarly, for HIER2, we observed that the Sr isotope signatures of the four hulled barley samples were outside the external reproducibility of ± 0.00003 (from 0.7080 to 0.70847), as were the $\delta^{88/86}$Sr values (from -0.252 to -0.320 ‰) (Table 2).

The samples most concentrated in Ca corresponded to the chalk leachates (between 674 for a CONV sample and 794 µmol.g^{-1} for a HIER 2 sample). The least concentrated sample was the atmospheric deposition sample (0.085 ± 0.009 µmol.g^{-1}, 2SE, N=1). The ash and hulled barley samples from HIER 2 had the second highest values (216 ± 17.8 µmol.g^{-1}, 2SD, N=2), followed by non-EP soil leachates (104.3 ± 76.9 µmol.g^{-1}, 2SD, N=3), loess leachate and residue and soil residues (43.8 ± 15.92 µmol.g^{-1}, 2SD, N=9). Cereal organs had among the lowest Ca concentrations (16.4 ± 26.2 µmol.g^{-1}, 2SD, N=25), followed by EP soil leachates (2.62 ± 0.73 µmol.g^{-1}, 2SD, N=4) and chalk residues (0.97 ± 0.24 µmol.g^{-1}, 2SD, N=4).

For Na, the most concentrated samples were the loess and soil residues and ash (284 ± 77 µmol.g^{-1}, 2 SD, N=9), and the least concentrated sample was atmospheric deposition (0.043 ± 0.004 µmol.g^{-1}, 2SE, N=1). All the other samples had values between 0.20 and 8.71 µmol.g^{-1}.

The highest Sr concentrations were measured in chalk leachates (7.055 ± 5.15 µmol.g^{-1}, 2SD, N=4), followed by ash (1.11 ± 0.11 µmol.g^{-1}, 2SE, N=1), the loess leachate and residues and soil residues (0. 661 ± 0.318 µmol.g^{-1}, 2SD, N=9), hulled barley from HIER 2, then soil leachates - except from EP (0.177 ± 0.162 µmol.g^{-1}, 2SD, N=4), soil leachates from EP, chalk residues and all plant organs (0.024 ± 0.044 µmol.g^{-1}, 2SD, N=33). Again, atmospheric deposition had the lowest Sr concentrations (0.00016 ± 0.00001 µmol.g^{-1}, 2SE, N=1).

4. Discussion

4.1 Ca-Sr analogy

The $^{87}Sr/^{86}Sr$ isotope and the Ca/Sr elemental ratios are classic indirect tracers of the Ca sources in natural ecosystems. Indeed, Ca and Sr are alkaline cations and their biogeochemical cycles are often assumed to be similar due to their similar ionic radius (r_{Sr} = 0.113 nm and r_{Ca} = 0.099 nm) and divalent charge (e.g. Poszwa et al., 2000; Probst et al., 2000) The $^{87}Sr/^{86}Sr$ isotope ratio is a valid source tracer since ^{87}Sr results from the radioactive decay of ^{87}Rb. Furthermore, this ratio is not affected by mass fractionation during continental weathering or biological processes since the fractionation is small and is circumvented via internal normalisation during the measurement process. Therefore, the $^{87}Sr/^{86}Sr$ isotope ratio has often been used in biogeochemical studies in forest ecosystems to determine the sources of Ca (and their mixtures) available to forests (atmosphere, shallow organic soils or deeper organic and mineral soils) (e.g. Åberg et al., 1990; Miller et al., 1993; Bailey et al., 1996; Blum et al., 2002; Kennedy et al., 2002; Bélanger et al., 2012). Furthermore, the Ca/Sr elemental ratio has also been proposed as a tool to trace Ca sources and fluxes in forest ecosystems, for which the fractionation between Ca and Sr during biogeochemical processes is not significant and/or is constrained by an appropriate discrimination factor (e.g. Poszwa et al., 2000; Blum et al., 2002; Poszwa et al., 2004; Blum et al., 2008; Drouet and Herbauts, 2008; Pett-Ridge et al., 2009).

In our study, the different samples followed two trends. The first was characterised by a relatively constant molar Ca/Sr ratio below 200 (µmol/g)/(µmol/g) and a $^{87}Sr/^{86}Sr$ ratio varying between 0.70739 and 0.73423. This was the case for soils (leachate and residues), loess (leachate and residues), chalk (residues) and ash (Fig. 4a). The second trend showed strong variations in the molar Ca/Sr ratio, between 77 and 2872 (µmol/g)/(µmol/g), and low variability in the $^{87}Sr/^{86}Sr$ ratio with a value less than 0.71178. This was the case for all the other samples, including the cereal samples. This suggests a chemical and biological fractionation between Ca and Sr, previously observed elsewhere (e.g. Bailey et al., 1996; Capo et al., 1998; Chadwick et al., 1999; Poszwa et al., 2000; Dasch et al., 2006; Blum et al., 2008; Drouet and Herbauts,

2008). Only the bread wheat organs, except for grains, showed a positive correlation between $^{87}Sr/^{86}Sr$ and Ca/Sr (Fig. 4b) (see Discussion, paragraph 4.2).

To circumvent this problem, many studies have directly applied stable Ca isotopes in addition to radiogenic Sr isotopes to trace Ca sources and underlying mechanisms (e.g. Cenki-Tok et al. 2009; Bagard et al., 2013; Schmitt et al., 2017). More recently, other studies have tested the potential of combining the stable Ca and Sr isotope approaches (Böhm et al., 2012; Bullen and Chadwick, 2016 ; Wang et al., 2019, 2021 ; Brazier et al., 2020a ; Nitzsche et al., 2022). We have seen that $\delta^{88/86}Sr$ and $\delta^{44/40}Ca$ were positively correlated (Fig. 5a; $R^2= 0.88$, $p<0.0001$) in the present study, with a slope of 0.29.

This agrees with the results obtained by other studies combining these two stable isotope systems. If we plot the linear trends observed in these previous studies, we see two families of trends: most samples plot along a slope between 0.13 and 0.29, similar to this study and few others plot along a slope between 3.17 and 3.19 (Figure 5b). Three studies presenting a low slope looked at precipitation of inorganic calcite under controlled conditions; they assert that the positive correlation observed between $\delta^{88/86}Sr$ and $\delta^{44/40}Ca$ was due to a kinetic control occurring during the dehydration of the Sr^{2+} and Ca^{2+} aqua complexes, involving varying mass fractionations between carbonates and seawater, rather than due to mixing between different mixing end-member (Böhm et al., 2012; Wang et al., 2019; 2021). Samples of lava and tephra, vegetation, the soil fraction holding available water and the total exchangeable fraction for Hawaiian soils also correlated with a low slope (Bullen and Chadwick, 1996), of the same order of magnitude as the present study (0.22 and 0.29, respectively). In contrast, the exchangeable fraction at 0.1N N-ammonium acetate from the same Bullen and Chadwick study had a higher slope, similar to that obtained for aquatic macroinvertebrates and small gobies (Nitzsche et al., 2022) (3.17 and 3.19, respectively). The latter authors interpreted this positive correlation as reflecting similar Ca and Sr sources leading to similar fractionation mechanisms.

Some samples do not show any correlation; for example, in a study that focused on understanding the formation of roots encrusted with $CaCO_3$ (rhizoliths) in loess-paleosol sequences, the authors suggested differences in the Ca and Sr sources, or their proportions during their formation (Brazier et al., 2020b). In the study by Nitzsche et al. (2022), some samples did not show a correlation between $\delta^{88/86}Sr$ and $\delta^{44/40}Ca$ (leaf-shredding crane fly larvae and goby bones), also suggesting a decoupling of Ca and Sr sources.

To summarize the current state of knowledge, by analogy with what is known for other isotopic systems, e.g. δD-$\delta^{18}O$, $\delta^{15}N$-$\delta^{13}C$ or $\delta^{24}Mg$-$\delta^{11}Li$, we propose that linear correlations reflect fractionations linked to either processes or mixtures (e.g. Cooper et al., 1991 ; Tipper et al., 2012 ; Phillips et al., 2014 ; Vander-Zanden et al., 2016).

The different slopes and intercepts can therefore be explained by system-dependent partition coefficients between Sr and Ca. More studies are now needed to understand the origin of these variations.

Because of the observed $\delta^{88/86}Sr$ and $\delta^{44/40}Ca$ correlation, we infer that both stable isotope systems $\delta^{88/86}Sr$ and $\delta^{44/40}Ca$ give the same information and can be used interchangeably to analyse Ca fluxes in this study. Consequently, we will focus our discussion on $\delta^{88/86}Sr$ and $^{87}Sr/^{86}Sr$ in the following paragraphs.

4.2 Cereal organs

Variations in stable and radiogenic Sr isotope compositions were observed among different locations, at both an intraspecific (one cereal species, different organs of the same plant) and extra specific level (different cereal species), but also within caryopses of the same cereal species from different localities (Fig. 4b and 6). The variability in $^{87}Sr/^{86}Sr$ in the studied cereal organs was related to locality and not to the type of organ or cereal (Fig. 6a): the least radiogenic signatures were observed for HIER1, HIER2 and GOUZ; the most radiogenic for EP and CONV. Some samples from the latter two plots showed variable signatures between the two

extremes. For example, for bread wheat and emmer from EP, the leaf and straw organs, formed first, were less radiogenic than the caryopses, glumes or awns, formed later. These variations suggest a variation in the Sr reservoir from which the plant draws its nutrients during its growth, in agreement with the results obtained in previous studies (e.g. Drouet et al. 2005b, Souza et al., 2010, Styring et al., 2016, Schmitt et al. 2017; Guilbourdenche et al., 2021).

Souza et al. (2010) were the first to report stable Sr isotope fractionations during root absorption and translocation to higher organs. This process was recently confirmed in studies by Oeser and von Blankenburg (2020), and Guilboudenche et al. (2021). In our study, the highest amplitudes of $\delta^{88/86}$Sr isotope fractionations were observed between straw and awn samples on the one hand, and the other plant samples, on the other hand; the lowest variability was for caryopses. By analogy with what has been observed for Ca (bean seeds grown under controlled conditions are enriched in the light ^{40}Ca isotope, Cobert et al., 2011), we propose that this enrichment reflects the preferential incorporation of lighter isotopes (^{86}Sr and ^{40}Ca) in calcium oxalate crystals (Schmitt et al., 2018). For organs other than caryopses, it is more complicated to propose an interpretation, since the stable isotope fractionation was accompanied by variations in ^{87}Sr/^{86}Sr, even for a given cereal species at a given location. The variability of the isotopic fractionation could therefore be linked to either biological fractionation and/or to a variation in the source impacting the biological fractionation. Therefore, we focused on seed samples of different cereals. In order to limit the observed inter-grain variations (Table 2), we systematically analysed batches of 10 caryopses. It should also be noted that grains are the organs most frequently found in ancient plant remains.

4.3 Sources of Sr from grains

The samples varied between two end-member, a silicate one (including soil leachates from the EP plot, all soil and chalk residues), and a carbonate one (including chalk, loess and soil

leachates from GOUZ, HIER1, but also grains grown on HIER1, HIER 2 and GOUZ) (Fig. 7). The other samples (loess residue, ash, atmospheric deposits, EP and CONV caryopses) were slightly more radiogenic than the carbonate end-member though the values were still close (Fig. 7).

Combining the $\delta^{88/86}Sr$ and $^{87}Sr/^{86}Sr$ measurements showed that the samples were predominantly governed by a source variation between a carbonate and a silicate end-member, and not by an isotopic fractionation process (Fig. 8). Soil and chalk residues and EP soil leachates were characterized by a silicate source and isotopic fractionation, with leachates enriched in ^{86}Sr relative to residues, which were enriched in ^{88}Sr, in agreement with previous studies (e.g. Chao et al., 2015; Stevenson et al., 2018; Yoshimura et al., 2021). This fractionation could be interpreted as preferential adsorption of the lighter isotope ^{86}Sr onto secondary soil minerals such as phyllosilicates, which has been observed for other isotopic systems such as Ca (Brazier et al., 2019).

It can be compared that in contrast to the soil leachates, the residues of all studied soils show higher $^{87}Sr/^{86}Sr$ values, indicating a silicate source (Fig. 8). Leachates from freshly cleared EP soils were all in the silicate end-member, unlike those from the chalk-amended soils which tended towards the carbonate end-member. Following equation (3), a simple mixing calculation for Sr between the mean value of the EP leachates and the leachates of chalk applied to each field suggests that the soils at HIER 1, HIER 2 and GOUZ respectively reflect 90, 82 and 94% of the contribution of the carbonate fraction of the chalk used as an amendment. The caryopses showed variability in $^{87}Sr/^{86}Sr$ depending on the field they were from: the most radiogenic samples were from the EP plot (0.7119 ± 0.0003, N=7), the least radiogenic were from HIER 1, HIER 2 and GOUZ (0.7082 ± 0.04, N=7), and the sample from the CONV plot had an intermediate value. A mixed calculation between the mean values of chalk leachate and soils from HIER 1, HIER 2 and GOUZ suggests that the seeds reflect 97% ± 1% (2SD, N=7) for

HIER 1, HIER 2 and GOUZ, and 92% (N=1) for CONV of a chalk leachate type signature. This agrees with the literature: the older the marling activity, the more calcium and carbonate there is in the soil (Goulding et al., 2016), which is reflected in the grains.

The cereals from the EP plot show low radiogenic signatures compared to what would be expected from the values for the soils on which they grew (Fig. 8). It should also be noted that the ash (0.72545 ± 0.00001, N=1) from trees grown on the EP plot was also less radiogenic than the EP plot soils, but more so than the cereal grains grown after thinning the forest plot. Other studies in a forest environment on acidic soil in the Vosges mountains in France have shown Sr isotope compositions in plants that are less radiogenic than in the soils (or soil leachates) on which they grew (Schmitt et al., 2017; Chabaux et al., 2019). In such a case the authors suggested an influence not of the bulk soil or soil leachates, but of the soil solution, or directly from specific primary or secondary mineral phases (apatite, plagioclase, clay minerals, oxide-hydroxides...), which are less radiogenic than the bulk soil. Farkaš et al. (2011) confirmed that roots can bypass the exchange complex to take up nutrients. Indeed, their study shows that roots remove nutrients from wet atmospheric deposits, complexed organically in forest soils, as well as from the dissolution of apatite and plagioclase. More recently, Uhlig et al. (2022) confirmed this decoupling and showed that in a forest ecosystem, plant tissues and organic matter had a Sr isotope signature similar to that of the biologically available calcium-bound P fraction. Such reservoirs could explain the lower $^{87}Sr/^{86}Sr$ signatures of plant organs compared to soils in our study.

In this case, a change in the nutrient reservoir or in the proportion of the nutrient reservoir when the trees were replaced by cereals must be considered. This could be explained in particular by the different rooting architectures of the different types of vegetation; the tree and cereal roots would draw nutrients from different soil reservoirs. Previous studies have focused on forest ecosystems developed on a granitic bedrock, which excludes any direct comparison with the

results of the present study (e.g. Schmitt et al., 2017; Chabaux et al., 2019; Farkaš et al. 2011; Uhlig et al., 2022). Additional studies including detailed investigations of the primary and secondary mineralogical phases of the luvisol and their Sr isotope compositions will likely be necessary to answer this question.

The observed difference in $^{87}Sr/^{86}Sr$ signatures could also be explained by the different life cycle of trees and cereals: trees integrate nutrient sources over their entire life cycle, which is much longer than that of a cereal. A change in source could therefore also have affected the trees, but would not have been visible in the ash, resulting from a combination of different species and containing elements accumulated over the whole life of the different trees. A fine study of the different root types could identify the sources of this variability, since the fine roots in trees are responsible for the current uptake of nutrients (over a season or up to a year), whereas the large and medium roots reflect older nutrient sources (Schmitt et al., 2017). The $^{87}Sr/^{86}Sr$ isotope variability within different EP cereal organs points to some heterogeneity in nutrient sources, but all of these organs remain less radiogenic than the ash (c.f. paragraph 4.2 and Fig. 6).

The proportions of carbonate sources could also vary over space and time. However, luvisol is decarbonated and there were no outcrops of carbonates on the experimental plot. On the other hand, chalk was spread in the neighbouring fields (including the CONV field). Chalk dust could therefore have blown away and been deposited via dry or wet atmospheric deposition on the soils in the Bois d'Arrouaise. Furthermore, the local geological map (Celet et al, 1979) and cartographic compilation work (Lehmkuhl et al, 2021) report thick loessic formations (aeolian silt) in the area where the experimental plot is located. As the isotopic signatures of the chalk are close to those of the loess sampled in the study area, it is impossible to distinguish between these two sources. Furthermore, it should be noted that the isotopic signature of the atmospheric inputs in Sr (stable and radiogenic) was compatible with a carbonate signature. This was the

signature of the dissolved fraction, suggesting that a loess, a marled soil and/or a chalk fraction was dissolved there. However, given the very low concentrations of Ca (85 nmol/L) and Sr (0.16 nmol/L), the dissolved fraction is unlikely to be their main source; atmospheric dust is a more likely candidate. Numerous studies have highlighted the role of forests, and more generally of vegetation, in preventing soil erosion, but also in retaining dust particles carried by the wind (e.g. Grousset and Biscaye, 2005; Yan et al., 2011 and refs; Lequy et al., 2012; Wei et al., 2020). We therefore assume that local atmospheric dust volumes have recently increased, and are now trapped in the local forest environment sheltered from the wind. This increase in airborne dust could be due to the clearing of land (late 19th century, 1960s) and the subsequent conversion of grazing land and pastures to agriculture (early 1990s). Bare silty agricultural land is known to produce large volumes of dust (Katra et al, 2016). This could contribute about 30 % of the carbonate fraction to the ash, and the percentage could increase to 75 ± 2 % (2SD, N=7) or 85% ± 2 % (2SD, N=7), depending on whether the end-member was the leachate from the chalk or loess or the leachate from the EP soils for the EP caryopses. These results are consistent with those of Drouet et al. (2005a), who showed that, in the Ardennes forests on acidic bedrock adjacent to our experimental plot, the origin of Sr was ~ 40% atmospheric.

4.4 Tracing potential alkaline amendments for plant husbandry history

From the beginnings of agriculture from the Neolithic to the Iron Age, the evolution of alkaline amendment practices is still poorly known (e.g. Mazoyet and Roudard, 1997; Vannière and Martineau, 2005; Neveu et al, 2021). In the temperate forests of northern France and Europe, the practice of spreading ash is suspected to date back to the Neolithic period and may have continued in some cases into the Middle Ages. The first farmers cleared forest land to plant food crops and to graze their livestock (e.g. Iversen, 1956; Huttunen, 1980; Vuorela, 1986; Vannière and Martineau, 2005).

In order to rectify soil pH, the farmers used alkaline amendments, although it is not known which ones were used when and where (plant ash or local limestone). From the results of the present-day reference frame, we can deduce that we could transpose the results obtained on grains grown on haplic luvisols to similar terrains, such as for example the loess cover in the Paris basin, provided that they are not affected by diagenetic or post-formation alteration phenomena (e.g. Cerling, 1984; Amandson et al., 1994; Budd et al., 2002; Brazier et al., 2020a)

more radiogenic signatures of cereal grains reflect a more important silicate influence while less radiogenic signatures reflect a carbonate influence. We propose that a silicate influence would correspond more to an ashy amendment while a carbonate influence would indicate a marling/chalking type of amendment. Studying caryopses of different spatial and temporal origins covering the period from the beginning of the Neolithic (from 5600 to 2100 years BC) to Antiquity (from 52 BC to 476 AD) would allow us to verify if there was a spatial and/or temporal homogeneity in these practices and would clarify the transition from one technique to another.

Based on a predefined geological context, the results of our study concern a set of plants grown on luvisols derived from the weathering of thick loess formations in the humid temperate climate of Northern France. Under these conditions, we identified less radiogenic signatures in plant organs than in the soils or their leachates, indicating either (1) a change in the nutrient reservoirs within soils over time, or in their proportion, or (2) a variable contribution of atmospheric inputs of carbonate origin.

During the formation and evolution of luvisols from loessic deposits, many secondary minerals that are more or less radiogenic in Sr (e.g. iron oxides, clay minerals), can change in abundance, thus leading to differences in isotopic signatures within the non-carbonate fraction, and within the plants that will develop from these soils.

In the Neolithic period, people cultivated small plots of land. Even though a change in land use from forest cover to cultivated fields has been confirmed by observations of soil erosion as early as 4000 yrs BP (Jenny et al., 2019), it is estimated that until 1000 BC, most of northwestern Europe was still forested (Kirby and Watkins, 1998; Foster et al., 2003; Egan and Howell, 2005; Dutoit et al., 2009). We can therefore assume that the wind erosion of soils at that time was less important than it is today. Indeed, vegetation cover was more extensive, there were fewer outcroppings of carbonate rocks (e.g. chalk), and surface areas of bare soil subject to deflation were also smaller. In contrast to today's situation, atmospheric deposition (from the wind deflation of carbonate loose particles) must have been much lower in the early days of agriculture. Therefore, it would be logical to obtain more radiogenic signatures on cereal grains in the case of ash amendments on fields in the past.

5. Conclusion

We identified a positive correlation between $\delta^{88/86}Sr$ and $\delta^{44/40}Ca$ of the samples, suggesting that Ca and Sr are from similar mass-dependent isotope sources and had undergone similar fractionation mechanisms. Intra-organ variability in cereals was also observed, reflecting variability in the nutrient source during the plant growth cycle as well as biological fractionation. Caryopses consistently had the most enriched signatures of the lighter Sr isotope (^{86}Sr), which may suggest that Sr is related to the precipitation of Ca oxalates. To limit inter- and intra-organ variability, we focused our study on samples of 10 caryopses for each cereal sample analysed.

From our study, it appears that the ash-amended grains are more radiogenic than the marled (with chalk) ones but less so than the soil leachates or the ash itself from the experimental plot. This can be explained in two ways: (1) either the source of Sr varied, or the proportion of several different sources varied, and/or (2) atmospheric inputs of carbonated dust were involved. For

cereals grown on loessic luvisols, our study showed a more radiogenic grain signature if ash from local wood had been applied. The Sr isotope signature was less radiogenic in the case of calcareous amendments (marling). Applying measurements of radiogenic Sr isotopes to archaeological cereal grains (from the Neolithic to the modern period) grown in similar environments as in this study and not affected by diagenesis, should therefore make it possible to identify ancient alkaline amendment practices. This type of analysis deployed in similar contexts (>2m thick siliceous soil cover, calcareous substrate and humid climate) and on large numbers of archaeological plant remains would make it possible to identify the spatial and temporal variability in the different amendment practices and would reveal potential transitions from one technique to another.

Bibliography

Abali, Y., Bayca, S.U., Arisoy, K., Vaizogullar, A.I. (2011) Optimization of dolomite ore leaching in hydrochloric acid solutions. Physicochem. Probl. Mineral Process. 46 (1), 253–262.

Åberg G., Jacksa G., Wickman T., Hamilton P.J. (1990) Strontium isotopes in trees as an indicator for calcium availability. Catena 17 (1), 1-11, doi: 10.1016/0341-8162(90)90011-2.

Amundson, R., Wang, Y., Chadwick, O., Trumbore, S., McFadden, L., McDonald, E., Wells, S., Deniro, M. (1994) Factors and processes governing the ^{14}C content of carbonate in desert soils. Earth Planet. Sci. Lett. 125 (1–4), 385–405.

Andrews, M.G., Jacobson, A.D., Lehn, G.O., Horton, T.W., Craw, D. (2016) Radiogenic and stable Sr isotope ratios ($^{87}Sr/^{86}Sr$, $\delta^{88/86}Sr$) as tracers of riverine cation sources and biogeochemical cycling in the Milford Sound region of Fiordland, New Zealand. Geochim. Cosmochim. Acta 173, 284–303.

Antoine P., Rousseau D.D., Zöller L., Lang A., Munaut A.V., Hatté C., Fontugne M. (2001) High-resolution record of the last interglacial-glacial cycle in the Nussloch loess-palaeosol sequences, Upper Rhine area, Germany, Quat. Int. 76, 211-229

Antoine P., Coutard S., Guerin G., Deschodt L., Goval E., Locht J.L., Paris C. (2016) Upper Pleistocene loess-palaeosol records from Northern France in the European context: Environmental background and dating of the Middle Palaeolithic. Quat Int 411, 4–24.

Arunakumara K.K.I.U., Walpola B.C., Yoon M.-H. (2013) Aluminum toxicity and tolerance mechanism in cereals and legumes — A review. J Korean Soc Appl Biol Chem 56, 1–9.

Bagard M.-L., Schmitt A.-D., Chabaux F., Pokrovsky O.S., Viers J., Stille P., Labolle F., Prokushkin A.S. (2013) Biogeochemistry of stable Ca and radiogenic Sr isotopes in a larch-covered permafrost-dominated watershed of Central Siberia, Geochim. Cosmochim. Acta 114, 169-187.

Bailey S.W., Hornbeck J.W., Driscoll C.T., Gaudette H.E. (1996) Calcium inputs and transport in a base-poor forest ecosystem as interpreted by Sr isotopes. Water Resour. Res. 32, 707–719.

Bélanger N., Holmden C., Courchesne F., Cote B.**, Hendershot W.H.** (2012) Constraining soil mineral weathering $^{87}Sr/^{86}Sr$ for calcium apportionment studies of a deciduous forest growing on soils developed from granitoid igneous rocks. Geoderma 185, 84-96.

Benson, L. V. (2012) Development and application of methods used to source prehistoric southwestern maize: a review, Journal of Archaeological Science, 39, 791–807.

Blum J.D., Dasch A.A., Hamburg S.P., Yanai R.D., Arthur M.A. (2008) Use of foliar Ca/Sr discrimination and $^{87}Sr/^{86}Sr$ ratios to determine soil Ca sources to sugar maple foliage in a northern hardwood forest. Biogeochem. 87, 287-296.

Blum J.D., Klaue A., Nezat C.A., Driscoll C.T., Johnson C.E., Siccama T.G., Eagar C., Fahey T.J., Likens G.E. (2002) Mycorrhizal weathering of apatite as an important calcium source in base-poor forest ecosystems. Nature 417, 729-731.

Böhm F., Eisenhauer A., Tang Jianwu, Dietzel M., Krabbenhöft A., Kisakürek B., Horn Ch., (2012) Strontium isotope fractionation of planktic foraminifera and inorganic calcite, Geochim. Cosmochim. Acta 93, 300-314.

Bouchez J., von Blanckenburg F. (2021) The rôle of vegetation in setting strontium stable isotope ratios in the critical zone, Am. J. Sci. Pp 1246-1283.

Brasseur B., Spicher F., Lenoir J., Gallet-Moron E., Buridant J., Horen H. (2018) What deep-soil profiles can teach us on deep-time pH dynamics after land use change? Land Degradation & Development. 29 (9) 2951-2961, doi: 10.1002/ldr.3065.

Brazier, J.M., Schmitt, A.D., Gangloff, S., Pelt, E., Chabaux, F., Tertre, E. (2019) Calcium isotopic fractionation during adsorption onto and desorption from soil phyllosilicates (kaolinite, montmorillonite and muscovite). Geochim. Cosmochim. Acta 250, 324–347.

Brazier J.-M., Schmitt A.-D., Gangloff S., Pelt E., Gocke I. M., Wiesenberg G.-L.B. (2020a) Multi-isotope approach ($\delta^{44/40}Ca$, $\delta^{88/86}Sr$ and $^{87}Sr/^{86}Sr$) provides insights into rhizolith formation mechanisms in terrestrial sediments of Nussloch (Germany), Chemical Geology 545, 119641. doi: 10.1016/j.chemgeo.2020.119641

Brazier, J.-M., Schmitt, A.-D., Pelt, E., Lemarchand, D., Gangloff, S., Tacail, T., Balter, V. (2020b) Determination of radiogenic $^{87}Sr/^{86}Sr$ and stable $\delta^{88/86}Sr_{SRM987}$ isotope values of thirteen mineral, vegetal and animal reference materials by DS-TIMS. Geostand. Geoanal. Res. https://doi.org/10.1111/ggr.12308.

Budd, D.A., Pack, S.M., Fogel, M.L. (2002) The destruction of paleoclimatic isotopic signals in Pleistocene carbonate soil nodules of Western Australia. Palaeogeogr. Palaeoclimatol. Palaeoecol. 188 (3–4), 249–273.

Bullen, T.D., Bailey, S.W. (2005) Identifying calcium sources at an acid deposition-impacted spruce forest: a strontium isotope, alkaline earth element multi-tracer approach. Biogeochemistry 74 (1), 63–99.

Bullen Th., Chadwick O. (2016) Ca, Sr and Ba stable isotopes reveal the fate of soil nutrients along a tropical climosequence in Hawaii. Chemical Geology 422, 25–45.

Capo R.C., Stewart B.W., Chadwick O.A. (1998) Strontium isotopes as tracers of ecosystem processes: theory and methods. Geoderma 82, 197–225, doi :10.1016/ S0016-7061(97)00102-X

Celet P., Maucorps P., Pomerol C., Rouil O., Solau J.L. (1979) Carte Geologique 1/50000eme : Feuille de Guise. Bureau de recherches geologiques et minieres.

Cenki-Tok B., Chabaux F., Lemarchand D., Schmitt A.-D., Pierret M.C., Viville D., Bagard M.L, Stille P. (2009) The impact of water-rock interaction and vegetation on calcium isotope fractionation in soil- and stream waters of a small, forested catchment (the Strengbach case). Geochim. Cosmochim. Acta 73, 2215-2228.

Cerling, T.E. (1984) The stable isotopic composition of modern soil carbonate and its relationship to climate. Earth Planet. Sci. Lett. 71 (2), 229–240.

Chabaux F., Stille P., Prunier J., Gangloff S., Lemarchand D., Morvan G., Négrel J., Pelt E., Pierret M.-C., Rihs S., Schmitt A.-D., Trémolières M., Viville D. (2019) Plant-soil-water interactions: implications from U-Th-Ra isotope analysis in soils, soil solutions and vegetation (Strengbach CZO, France). Geochim. Cosmochim. *Acta*, 259, 188-210.

Chadwick O.A., Derry L., Vitousek P.M., Huebert B.J., Hedin L.O. (1999) Changing sources of nutrients during four million years of ecosystem development. Nature 397, 491–497.

Chao H.-C., You C.-F., Liu H.-C., Chung C.-H. (2015) Evidence for stable Sr isotope fractionation by silicate weathering in a small sedimentary watershed in southwestern Taiwan, Geochim. Cosmochim. Acta 165, 324-341

Clow, D.W., Mast, M.A., Bullen, T.D., Turk, J.T. (1997) Strontium 87/strontium 86 as a tracer of mineral weathering reactions and calcium sources in an alpine/subalpine watershed, Loch Vale, Colorado. Water Resour. Res. 33 (6), 1335–1351.

Clout H.D., Phillips A.D.M. (1972) Fertilisants minéraux en France au XIXe siècle. Études rurales 45, 9–28.

Cobert F., Schmitt A.D., Bourgeade P., Labolle F., Badot P.M., Chabaux F., Stille P., (2011). Experimental identification of Ca isotopic fractionations in higher plants, Geochimica et Cosmochimica Acta, Volume 75, Issue 19, p.5467-5482, ISSN 0016-7037, doi: 10.1016/j.gca.2011.06.032.

Cooper L.W., Olsen C.R., Solomon D.K., Larsen I.L., Cook R B., Grebmeier J.M. (1991) Stable isotopes of oxygen and natural and fallout radionuclides used for tracing runoff during snowmelt in an Arctic watershed. Water Res. Res., 27(9): 2171-2179.

Dasch A., Blum J.D., Eagar C., Fahey T.J., Driscoll C.T., Siccama T.G. (2006) The relative uptake of Ca and Sr into tree foliage using a whole-watershed calcium addition. Biogeochem. 80, 21-41.

Drouet Th., Herbauts J., Gruber W., Demaiffe D. (2005a) Strontium isotope composition as a tracer of calcium sources in two forest ecosystems in Belgium. Geoderma, vol. 126, p.203-223. doi: 10.1016/j.geoderma.2004.09.010

Drouet Th., Herbauts J., Demaiffe D. (2005b) Long-term records of strontium isotopic composition in tree rings suggest changes in forest calcium sources in the early 20th century. Global Change Biology 11, 1926–1940, doi:10.1111/j.1365-2486.2005.01034

Drouet Th., Herbauts J. (2008) Evaluation of the mobility and discrimination of Ca, Sr and Ba in forest ecosystems: consequence on the use of alkaline-earth element ratios as tracers of Ca. Plant Soil 302, 105–124. https://doi.org/10.1007/s11104-007-9459-2

Dutoit T., Thinon M., Talon B., Buisson E., Alard D. (2009). Sampling soil wood charcoals at a high spatial resolution: a new methodology to investigate the origin of grassland plant communities. J.Veget. Sci. 20, 349–358.

Ehrmann O., Biester H., Bogenrieder A., Rösch M. (2014) Fifteen years of the Forchtenberg experiment—results and implications for the understanding of Neolithic land use. Veget Hist Archaeobot 23, 5–18.

Egan D., Howell E.A. (2005). The Historical Ecology Handbook. Island Press.

Fachin P.A., Costa Y.T., Thomas E.L. (2021) Evolution of the soil chemical properties in slash-and-burn agriculture along several years of fallow. Sci. Tot. Env. 764, 142823.

Farkaš J., Déjeant A., Novák M., Jacobsen S.B. (2011) Calcium isotope constraints on the uptake and sources of Ca^{2+} in a base-poor forest: A new concept of combining stable ($\delta^{44/42}Ca$) and radiogenic (εCa) signals. Geochim. Cosmochim. Acta **75**, 7031-7046.

Foster D., Swanson F., Aber J., Burke I., Brokaw N., Tilman D., Knapp A. (2003). The importance of landuse legacies to ecology and conservation. BioScience, 53, 77–88.

Gosse A.A.J. (1786) Histoire de l'Abbaye et de l'ancienne Congregation des chanoines reguliers d'Arrouaise, avec des notes critiques, historiques et diplomatiques, imprime à Lille, chez Leonard Danel.

Goulding K. W. T. (2016) Soil acidification and the importance of liming agricultural soils with particular reference to the United Kingdom. Soil Use and Management, Volume 32, Issue 3 p. 390-399, doi: 10.1111/sum.12270

Goulding K.W.T., Annis B. (1998) Lime and liming in UK agriculture. Proceedings No 410. The Fertiliser Society. York, UK. p.36

Goulding K.W.T., McGrath S.P., Johnston A.E. (1989) Predicting the lime requirement of soils under permanent grassland and arable crops. Soil Use and Management, 5, 54–57. doi: 10.1111/j.1475-2743.1989.tb00760.x

Grousset F.E., Biscaye P.E., (2005). Tracing dust sources and transport patterns using Sr, Nd and Pb isotopes. Chem. Geol. 222, 149–167, doi: 10.1016/j.chemgeo.2005.05.006

Guibourdenche L., Stevenson R., Pedneault K., Poirier A., Widory D. (2020) Characterizing nutrient pathways in Quebec (Canada) vineyards: Insight from stable and radiogenic strontium isotopes, Chem. Geol. 532, 119375

Haesaerts P. (1984) Les formations fluviatiles pléistocènes du bassin de la Haine (Belgique), Quaternaire, 21-1-3, 19-26

Hajj F., Poszwaa A., Bouchez J., Guérolda F., (2017). Radiogenic and "stable" strontium isotopes in provenance studies: A review and first results on archaeological wood from shipwrecks. Journal of Archaeological Science, Volume 86, p. 24-49, doi: 10.1016/j.jas.2017.09.005

Heier, A., Evans, J. A., and Montgomery, J. (2009) The potential of carbonized grain to preserve biogenic $^{87}Sr/^{86}Sr$ signatures within the burial environment, Archaeometry, 51, 277–91.

Heuser A., Schmitt A.-D., Gussone N., Wombacher F. (2016) Analytical methods. In: Gussone N., Schmitt A.-D., Heuser A., Wombacher F., Dietzel M., Tipper E., Schiller M. "Calcium Stable Isotope Geochemistry", Springer, 23-73.

Hippler D., Schmitt A.-D., Gussone N., Heuser A, Stille P., Eisenhauer A., Nägler Th. F. (2003) Calcium isotopic composition of various reference materials and seawater, *Geostandard Newsletter* 27 (1), 13-19.

Huttunen P. (1980) « Early land use, especially the slashand-burn cultivation in the commune of Lammi, southern Finland, interpreted mainly using pollen and charcoal analyses », Ada Botanica Fennica, 113, p. 1-45.

Iversen J. (1956) « Forest clearance in the Stone Age », Scientific American, 194, p. 36-41.

Jenny J.-P., Koiralaa S., Gregory-Eavesc I., Francusd P., Niemanna C., Ahrensa B., Brovkinf V., Baud A., Ojalag A.E.K., Normanderau A., Zolitschkai B., Carvalhaisa N. (2019) Human and climate global-scale imprint on sediment, PNAS 116 (46), 22972-22976

Juo A.S.R., Manu A. (1996) Chemical dynamics in slash-and-burn agriculture. Agriculture, Ecosystems & Environment, Volume 58, Issue 1, p.49-60, doi; 10.1016/0167-8809(95)00656-7

Katra, I., Gross, A., Swet, N., Tanner S., Krasnov H., Angert A. (2016) Substantial dust loss of bioavailable phosphorus from agricultural soils. Sci Rep 6**,** 24736.

Kennedy M.J., Hedin L.O., Derry L.A. (2002) Decoupling of unpolluted temperate forests from rock nutrient sources revealed by natural $^{87}Sr/^{86}Sr$ and ^{84}Sr tracer addition. Proc. Natl. Acad. Sci. 99, 9639–9644.

Kirby K.J., Watkins C. (1998). The ecological history of European forests. Wallingford, UK, CAB International.

Larsson M., Magnell O., Styring A., Lagerås Per, Evans J. (2020) Movement of agricultural products in the Scandinavian Iron Age during the first millennium AD: $^{87}Sr/^{86}Sr$ values of archaeological crops and animals in southern Sweden, STAR: Science & Technology of Archaeological Research, 6:1, 96-112, DOI: 10.1080/20548923.2020.1840121

Läuchli A., Grattan S.R. (2017) Plant stress under non-optimal soil pH, in: Plant Stress Physiology, 2nd Edition. CABI, pp. 201–2016.

Lehmkuhl F., Nett J.J., Pötter S., Schulte P., Sprafke T., Jary Z., Antoine P., Wacha L., Wolf D., Zerboni A., Hösek J., Markovic S.B., Obrecht I., Sümegi P., Veres D., Zeeden C., Lehn G.O., Jacobson A.D. (2015) Optimization of a 48Ca–43Ca double-spike MC-TIMS method for measuring Ca isotope ratios (δ44/40Ca and δ44/42Ca): limitations from filament reservoir mixing, JAAS 30, 1571-1581

Lequy E., Conil S., Turpault M.-P. (2012) Impacts of Aeolian dust deposition on European forest sustainability: A review, Forest Ecol. Manag., DOI: 10.1016/j.foreco.2011.12.005

Liu H.C., Chung C.H., You C.F., Chiang Y.H. (2016) Determination of $^{87}Sr/^{86}Sr$ and $\delta^{88/86}Sr$ ratios in plant materials using MC-ICP-MS, Anal. Bioanal Chem 408, 387-397.

Marschner H. (1995) Mineral Nutrition of Higher Plants, 2nd edition. Academic Pres.

Matthew W.M. (1993) Marling in British agriculture: a case of partial identity. Agricultural History Review 41, 97–110.

Mazoyer M., Roudard L. (1997) Histoire des agricultures du monde : du néolithique à la crise contemporaine , Éditions du Seuil, 545p.

Miller E.K., Blum J.D., Friedland A.J., (1993) "Determination of soil exchangeable-cation loss and weathering rates using Sr isotopes". Nature 362, 438-441.

Nitzsche K.N., Wakaki S., Yamashita K., Shin K-C., Kato Y., Kamauchi H., Tayasu I. (2022) Calcium and strontium stable isotopes reveal similar behaviors of essential Ca and nonessential Sr in stream food webs, Ecosphere 13:e3921, doi.org/10.1002/ecs2.3921

Neveu E., Zech-Matterne V., Brun C., Dietsch-Sellami M.-F., Durand F., Toulemonde F. (2021) New insights into agriculture in northwestern France from the Bronze Age to the Late Iron Age: a weed ecological approach. Veget Hist Archaeobot **30,** 47–61.

Oeser R.A., von Blanckenburg F. (2020) Strontium isotopes trace biological activity in the Critical Zone along a climate and vegetation gradient, Chem. Geol. 558, 119861

Palm C.A., Swift M.J., Wooler P. L. (1996) Soil biological dynamics in slash-and-burn spreading agriculture. Agriculture, Ecosystems & Environment, Volume 58, Issue 1, p. 61-74, doi: 10.1016/0167- 8809(95)00653-2

pPelt, E., Chabaux, F., Stille, P., Innocent, C., Ghaleb, B., Gérard, M., Guntzer, F. (2013) Atmospheric dust contribution to the budget of U-series nuclides in soils from the Mount Cameroon volcano. Chem. Geol. 341, 147–157.

Pett-Ridge J.C., Derry L.A., Kurtz A.C. (2009) Sr isotopes as a tracer of weathering processes and dust inputs in a tropical granitoid watershed, Luquillo Mountains, Puerto Rico Geochim. Cosmochim. Acta 73, 25-43.

Phillips D.L., Inger R., Bearhop S., Jackson A.L., Moore J.W., Parnell A.C., Semmens B.X., Ward E.J. (2014) Best practices for use of stable isotope mixing models in food-web studies Can. J. Zool. 92: 823–835 (2014) dx.doi.org/10.1139/cjz-2014-0127

Poszwa A., Dambrine E., Pollier B., Atteia O. (2000) A comparison between Ca and Sr cycling in forest ecosystems. Plant Soil 225, 299–310.

Poszwa A., Ferry B., Dambrine E., Pollier B., Wickman T., Loubet M., Bishop K. (2004) Variations of bioavailable Sr concentration and 87Sr/86Sr ratio in boreal forest ecosystems. Biogeochemistry 67, 1–20, doi : 10.1023/B:BIOG.0000015162.12857.3e

Poszwa A., Ferry B., Pollie B., Grimaldi C., Charles-Dominique P., Loubet M., Dambrine E. (2009) Variations of plant and soil $^{87}Sr/^{86}Sr$ along the slope of a tropical inselberg. Ann. For. Sci. 66, 512, DOI: 10.1051/forest/2009036

Probst, A., El Gh'mari, A., Aubert, D., Fritz, B., McNutt, R. (2000) Strontium as a tracer of weathering processes in a silicate catchment polluted by acid atmospheric inputs, Strengbach, France. Chem. Geol. 170 (1–4), 203–219.

Ritchie G.S.P. (1989). 1 - The Chemical Behaviour of Aluminium, Hydrogen and Manganese in Acid Soils, in: Robson, A.D. (Ed.), Soil Acidity and Plant Growth. Academic Press, pp. 1–60.

Rösch M., Biester H., Bogenrieder A., ckmeier E., hrmann O., Gerlach R., Hall M., Hartkopf-Fröder C., Herrmann L., Kury B., Lechterbeck J., Schier W., Schulz E. (2017) Late Neolithic Agriculture in Temperate Europe—A Long-Term Experimental Approach. Land 6, 11; doi:10.3390/land6010011

Schmitt, A.D., Cobert, F., Bourgeade, P., Ertlen, D., Labolle, F., Gangloff, S., Badot, P.M., Chabaux, F., Stille, P. (2013) Calcium isotope fractionation during plant growth under a limited nutrient supply. Geochim. Cosmochim. Acta 110, 70–83.

Schmitt, A.D., Gangloff, S., Labolle, F., Chabaux, F., Stille, P. (2017) Calcium biogeochemical cycle at the beech tree-soil solution interface from the Strengbach CZO (NE France): insights from stable Ca and radiogenic Sr isotopes. Geochim. Cosmochim. Acta 213, 91–109.

Schmitt A.D., Borrelli N., Ertlen D., Gangloff S., Chabaux F. (2018). Stable calcium isotope speciation and calcium oxalate pstrawuction within beech tree (Fagus sylvatica L.) organs. Biogeochemistry Volume 137, p. 197–217, doi:10.1007/s10533-017-0411-0

Scott B.J., Fisher J.A. (1989) 5 - Selection of Genotypes Tolerant of Aluminium and Manganese, in: Robson, A.D. (Ed.), Soil Acidity and Plant Growth. Academic Press, pp. 167–203

Schuessler J.A., von Blackenburg F., Bouchez J., Uhlig D., Hewawasam T. (2018) Nutrient cycling in a tropical montane rainforest under a supply-limited weathering regime traced by elemental mass balances and Mg stable isotopes, Chem. Geol. 497, 74-87

Shalev, N., Gavrieli, I., Halicz, L., Sandler, A., Stein, M., Lazar, B. (2017) Enrichment of ^{88}Sr in continental waters due to calcium carbonate precipitation. Earth Planet. Sci. Lett. 459, 381–393.

Snir A., Nadel D., Groman-Yaroslavski I., Melamed Y., Sternberg M., Bar-Yosef O., Weiss E. (2015) The Origin of Cultivation and Proto-Weeds, Long Before Neolithic Farming. PLOS ONE 10, e0131422. https://doi.org/10.1371/journal.pone.0131422

Styring A., Maier U., Stephan E., Schlichthele H., Bogaard A. (2016) Cultivation of choice: new insights into farming practices at Neolithic lakeshores sites. Antiquity 90, 349, 95-110.

Styring A.K., Evans J.A., Nitsch E.K., Lee-THorp J.A., Bogaard A. (2019) Revisiting the potential of carbonized caryopse to preserve biogenic $^{87}Sr/^{86}Sr$ signatures within the burial environment. Archaeom. 61 (1), 179-193.

Souza G. F., Reynolds B C., Kiczka M., Bourdon B., (2010). Evidence for mass-dependent isotopic fractionation of strontium in a glaciated granitic watershed. Geochimica et Cosmochimica Acta, Volume 74, Issue 9, p. 2596-2614, ISSN 0016-7037, doi: 10.1016/j.gca.2010.02.012

Stevenson, R., Pearce, C. R., Rosa, E., Hélie, J. F., and Hillaire-Marcel, C. (2018). Weathering processes, catchment geology and river management impacts on radiogenic

($^{87}Sr/^{86}Sr$) and stable ($\delta^{88/86}Sr$) strontium isotope compositions of Canadian boreal rivers. *Chem. Geol.* 486, 50–60. doi:10.1016/j.chemgeo.2018.03.039

Tipper E.T., Lemarchand E., Hindshaw R. S., Reynolds B.C., Bourdon B. (2012) Seasonal sensitivity of weathering processes: hints from magnesium isotopes in a glacial stream. Chem. Geol. 312–313, 80–92.

Uhlig, D., Amelung, W., von Blanckenburg, F. (2022). Mineral nutrients sourced in deep regolith sustain long-term nutrition of mountainous temperate forest ecosystems. Global Biogeochemical Cycles, 34, e2019GB006513. https://doi. org/10.1029/2019GB006513

Vander-Zanden H.B., Soto D.X., Bowen G.J., Hobson K.A. (2016) Expanding the Isotopic Toolbox: Applications of Hydrogen and Oxygen Stable Isotope Ratios to Food Web Studies, Front. Ecol. Evol., https://doi.org/10.3389/fevo.2016.00020

Van Ham-Meert A., Rodler A.S., Waight T.E., Daly A. (2020) Determining the Sr isotopic composition of waterlogged wood – Cleaning more is not always better, J. Archaeolog. Sci. 124, 105261

Van Ranst, E., De Conick, F., Tavernier, R., Langohr, R. (1982) Mineralogy in silty to loamy soils of central and high Belgium in respect to autochthonous and allochthonous materials. Bulletin de la Societe Belge de Geologie, 91(1): 27-44.

Vannière B., Martineau R. (2005) Histoire des feux et pratiques agraires du Néolithique à l'âge du Fer en région Centre (France) : implications territoriales, démographiques et environnementales. Gallia Préhistoire – Archéologie de la France préhistorique, CNRS Éditions, 2005, 47, pp.167-186.

Vuorela I. (1986) « Palynological evidence of slash-andburn cultivation in South Finland », in Behre K. E. (éd.), Anthropogenic indicators in pollen diagrams, Rotterdam, Balkema, p. 53-64.

Wang, J., Jacobson, A.D., Zhang, H., Ramezani, J., Sageman, B.B., Hurtgen, M.T., Bowring, S.A., and Shen, S.-Z. (2019) Coupled $\delta^{44/40}Ca$, $\delta^{88/86}Sr$, and $^{87}Sr/^{86}Sr$ geochemistry

across the end-Permian mass extinction event: Geochimica et Cosmochimica Acta, v. 262, p. 143–165, https://doi .org/10.1016/j.gca.2019.07.035.

Wang J., Jacobson A.D., Sageman B.B., Hurtgen M.T. (2021) Stable Ca and Sr isotopes support volcanically triggered biocalcification crisis during Oceanic Anoxic Event 1a, Geology 49, 515–519.

Wei W., Wang B., Niu X., (2020) Forest Roles in Particle Removal during Spring Dust Storms on Transport Path, Int. J. Environ. Res. Public Health 17(2), 478; https://doi.org/10.3390/ijerph17020478

Wei, G., Ma, J., Liu, Y., Xie, L., Lu, W., Deng, W., Ren, Z., Zeng, T., Yang, Y. (2013) Seasonal changes in the radiogenic and stable strontium isotopic composition of Xijiang River water: Implications for chemical weathering. Chem. Geol. 343, 67–75.

WRB (2006) World reference base for soil resources 2006. A framework for international classification, correlation and communication. <www.fao.org/3/a-a0510e.pdf>.

Yan Y., Xu Xingliang, Xin Xiaoping, Yang G., Wang X., Yan R., Chen B. (2011) Effect of vegetation coverage on aeolian dust accumulation in a semiarid steppe of northern China, Catena 87, 351-356

Yan H., Schmitt A.D., Liu Z., Gangloff S., Sun H., Chen J., Chabaux F. (2016) Calcium isotopic fractionation during travertine deposition under different hydrodynamic conditions: examples from Baishuitai (Yunnan, SW China). Chem. Geol. 426, 60–70.

Yoshimura T., Wakaki S., Kawahata H., Hossain H.M.Z., Manaka T., Suzuli A., Ishikawa T., Ohkouchi N. (2021) Stable Strontium Isotopic Compositions of River Water, Groundwater and Sediments From the Ganges–Brahmaputra–Meghna River System in Bangladesh, Front. Earth Sci. https://doi.org/10.3389/feart.2021.592062

Figures

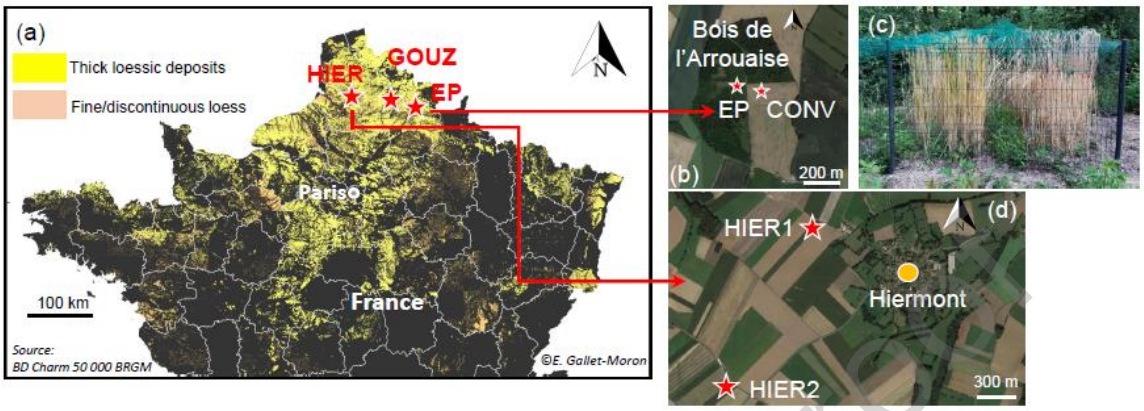

Fig.1: (a) Distribution of the silt deposits on bedrock in Northern France, and location of the study plots (Hiermont (HIER), Gouzeaucourt (GOUZ), Bois d'Arrouaise (EP)) (adapted from BD charm-50000-BRGM), (b) Location of the EP and CONV fields (© Google Earth), (c) Photograph of EP in July 2019 (© Brasseur), (d) Location of HIER1 and HIER 2 (© Google Earth).

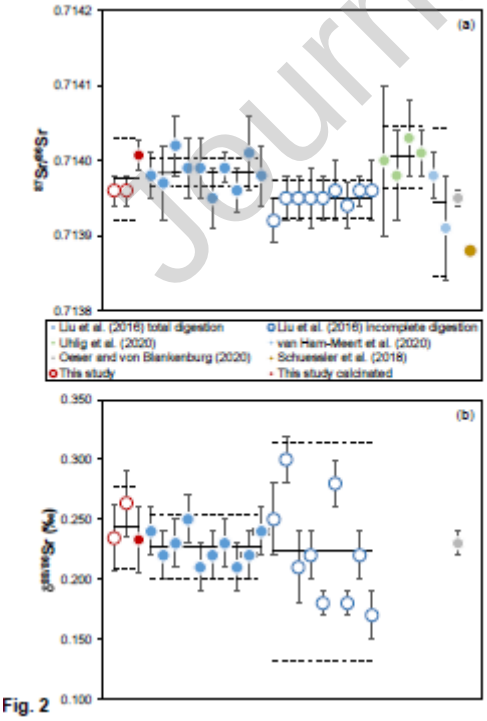

Fig. 2

Fig. 2: Isotopic compositions of (a) $^{87}Sr/^{86}Sr$ and (b) $\delta^{88/86}Sr$ for the NIST SRM1515 standard. The error bars assigned to each measurement point correspond to the internal error (2SE) and the mean values are those of each series of samples (solid lines) affected by the corresponding 2SD confidence interval (dotted lines)

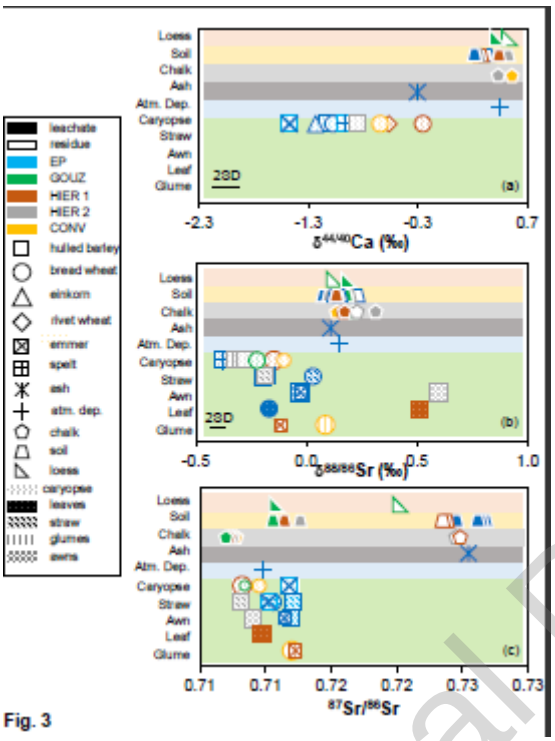

Fig. 3

Fig. 3: (a) $\delta^{44/40}Ca$ (‰), (b) $\delta^{88/86}Sr$ (‰) and (c) $^{87}Sr/^{86}Sr$ in the studied samples. For loess, soils and chalk, the coloured and empty symbols refer to leachates and residues, respectively. For cereal species, squares, circles, triangles, diamonds, framed crosses and framed pluses correspond respectively to hulled barley, bread wheat, einkorn, rivet wheat, emmer and spelt. The different fills correspond to different plant parts: small coloured dots on a white background = caryopses, small white dots on a coloured background = leaves, hatching = straw, grids = glumes and waves = awns. The different colours indicate location: blue, green, brown, grey and orange respectively represent EP, GOUZ, HIER 1, HIER 2 and CONV.

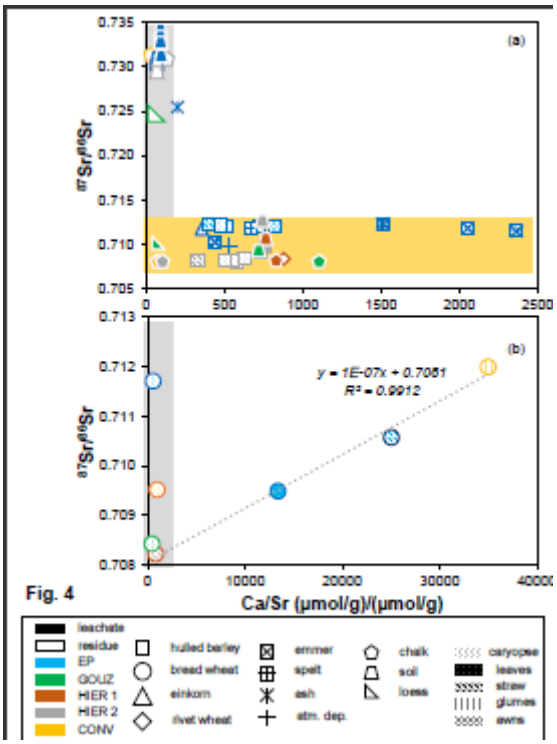

Fig. 4

Fig. 4: Variability in the $^{87}Sr/^{86}Sr$ versus molar Ca/Sr ratio for (a) all samples except (b) bread wheat. For loess, soils and chalk, the coloured and empty symbols respectively refer to leachates and residues. For cereal species, squares, circles, triangles, diamonds, framed crosses and framed pluses correspond to hulled barley, bread wheat, einkorn, rivet wheat, emmer and spelt, respectively. The different colours indicate location: blue, green, brown, grey and orange respectively represent EP, GOUZ, HIER 1, HIER 2 and CONV.

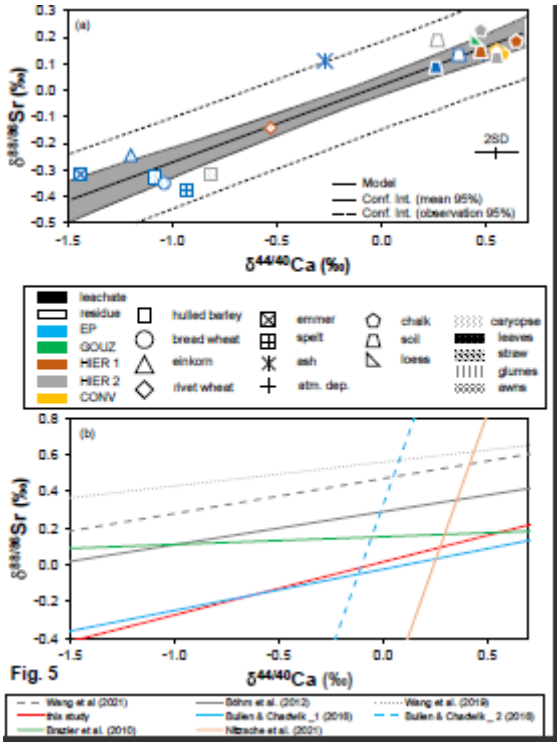

Fig. 5: Positive correlation between $\delta^{88/86}Sr$ and $\delta^{44/40}Ca$ (a) for the studied samples, and (b) for data from the literature. For soils, the coloured and empty symbols respectively refer to leachates and residues. For cereal caryopses, squares, circles, triangles, diamonds, framed crosses and framed pluses correspond to hulled barley, bread wheat, einkorn, rivet wheat, emmer and spelt, respectively. The different fills correspond to different plant parts: small coloured dots on a white background = caryopses, small white dots on a coloured background = leaves, hatching = straw, grids = glumes and waves = awns.

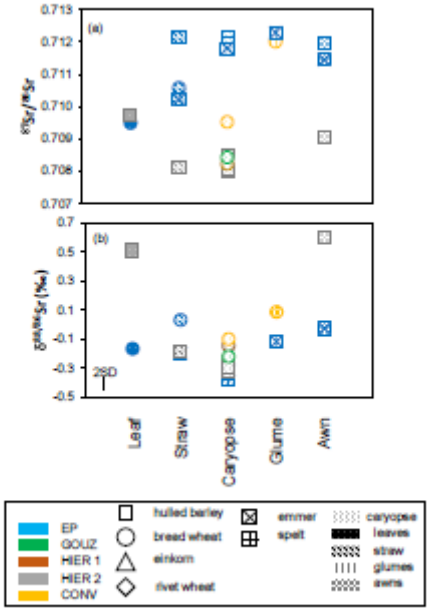

Fig. 6

Fig. 6: (a) $^{87}Sr/^{86}Sr$ and (b) $\delta^{88/86}Sr$ variations as a function of cereal organ. Error bars are within the size of the point. The different colours indicate location: blue, green, brown, grey and orange respectively represent EP, GOUZ, HIER 1, HIER 2 and CONV. The different fills correspond to different plant parts: small coloured dots on a white background = caryopses, small white dots on a coloured background = leaves, hatching = straw, grids = glumes and waves = awns.

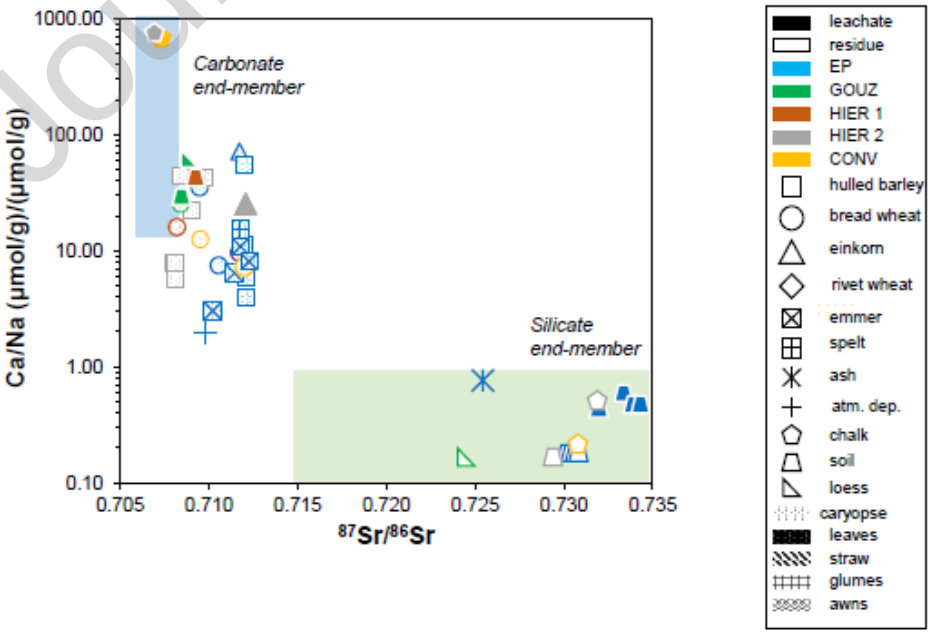

Fig. 7

Fig. 7: Molar Ca/Na versus $^{87}Sr/^{86}Sr$ for the studied samples. End-member values are from Meybeck (1986). For loess, soils and chalk, the coloured and empty symbols respectively refer to leachates and residues. For cereal caryopses, squares, circles, triangles, diamonds, framed crosses and framed pluses respectively correspond to hulled barley, bread wheat, einkorn, rivet wheat, emmer and spelt.

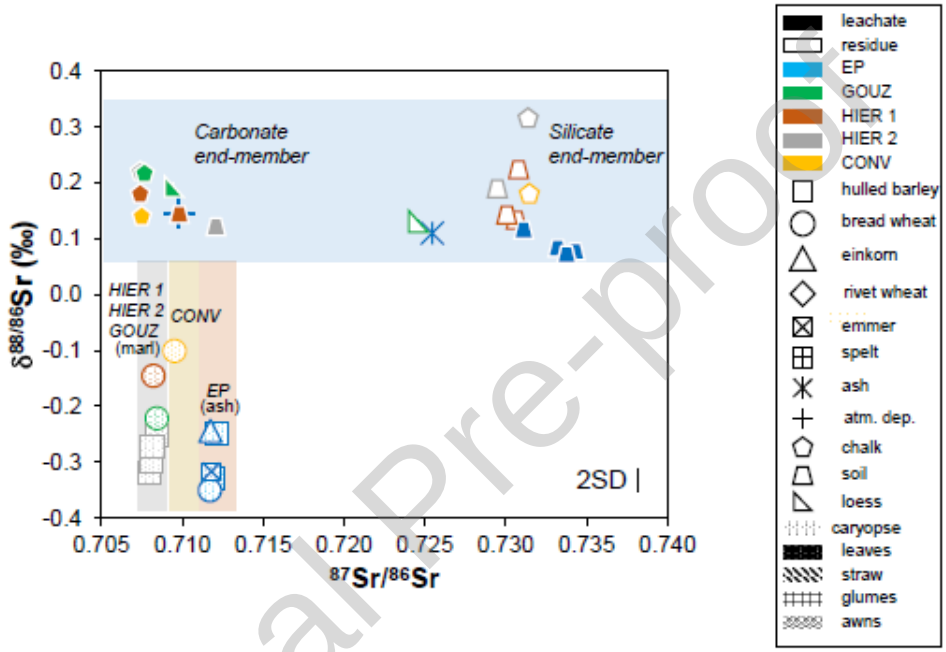

Fig. 8

Fig. 8: $\delta^{88/86}Sr$ (‰) as a function of $^{87}Sr/^{86}Sr$ for the studied samples. For loess, soils and chalk, the coloured and empty samples respectively refer to leachates and residues. For cereal organs, squares, circles, triangles, diamonds, framed crosses and framed pluses respectively correspond to hulled barley, bread wheat, einkorn, rivet wheat, emmer and spelt.

Tables

Table 1: Characteristics of the study sites

Short Name	Agricultural Practice	Location	Defore station date	Amendment type	Latitude	Longitude

EP	slash and burn experimental plot	Bois d'Arrouaise near the town of Rejet-de-Beaulieu	2018	burning (ash from spruce and oak trees cut on site)	N 50°1' 55.4118"	E 3°38' 0.801''
CONV	conventional agriculture field	100 m from the experimental plot, on the edge of the Bois d'Arrouaise	~ 1965	marling (chalk from the Paris Basin)	N 50°1' 54.4224"	E 3°38' 11.3094"
GOUZ	organic agriculture field	Gouzeaucourt	several centuries ago	"	N 50°3' 19.9794"	E 3°7' 26.148"
HIER 1	"	Hiermont	"	"	N 50°11' 55.3734"	E 2°3' 46.2774"
HIER 2	"	"	"	"	N 50°11' 16.8"	E 2°3' 32.0652"

Table 2: Stable Ca and Sr and radiogenic Sr isotopic composition of loess, soil, chalk, ash, atmospheric deposits and cereal organs. Subscripts 1 and 2 refer to replicates.

Sample ID	**Ref.**	**Location**	**Sample Type**	**Depth**	**Number of grains**	**Fraction**	**Ca**	**Na**	**Sr**	**$\delta^{88/86}Sr_1$**	**$\delta^{88/86}Sr_2$**	**$\delta^{44/40}Ca$**	**$^{87}Sr/^{86}Sr_1$**	**$^{87}Sr/^{86}Sr_2$**
				cm			*µmol/g*				*‰*			
LOl		GOUZ	loess			leachate	51.2	0.870	0.663	0.196	0.189	0.47	0.70940	
EPsl1		EP	soil	0-10		"	2.669	5.34	0.0026	0.085		0.26	0.73423	0.73423
EPsl2		"	"	20-30		"	2.996	5.77	0.0030	0.078		-0.00	0.73375	0.73376
EPsl3		"	"	45-55		"	2.10	4.46	0.0025	0.119		-0.00	0.73121	

EPsl4	"	"	95-105	"	2.70	4.08	0.028	0.085		-	0.73312	
HIER2sl	HIER2	"	0-10	"	89.7	3.55	0.121	0.124	0.109	0.56	0.71209	0.71209
HIER1sl	HIER1	"	0-10	"	75.2	1.65	0.100	0.142		0.48	0.70988	
GOUZsl	GOUZ	"	0-10	"	148	4.93	0.940	0.171		-	0.70903	
HIER2cl	HIER2	chalk	0-10	"	74.1	0.992	0.073	0.218		0.47	0.70739	
HIER1cl	HIER1	"	0-10	"	79.4	-7	8.51	0.175		0.62	0.70743	
GOUZcl	GOUZ	"	0-10	"	79.3	-3	3.23	0.221		-	0.70739	
CONVsl	CONV	"	0-10	"	67.4	0.970	8.65	0.140	0.140	0.60	0.70742	
LOr	GOUZ	loess		residue	59.5	3.47	0.896	0.128		0.56	0.72452	
EPsr1	EP	soil	0-10	"	40.5	2.83	0.677	0.142		0.37	0.73045	
EPsr2	"	"	20-30	"	42.8	2.97	0.707	0.137		-	0.73065	
EPsr3	"	"	45-55	"	44.8	3.07	0.748	0.226		-	0.73086	
EPsr4	"	"	95-105	"	45.8	2.96	0.752	-		-	0.73119	

HIER2		0-10		38.9	28	0.687	0.196		0.27	0.72959
HIER1		0-10		38.7	23	0.411	-		0.32	-
GOUZ		0-10		32.0	21	0.406	-		-	-
HIER2	chalk	0-10		1.02	2.30	0.011	0.313		-	0.73125
HIER1		0-10		1.02	1.57	0.034	-		-	-
GOUZ		0-10		0.798	3.57	0.034	-		-	-
CONV		0-10		1.05226	6.46	0.023	0.179		-	0.73144
Ash	EP	ash		2.20	2.90	1.11	0.110	0.073	-0.27	0.72545
Atm	"	atmospheric deposits		0.085	0.043	0.000	0.146		0.49	0.70980
EPbg10_1	OR2	"	hulled barley	10	carypose	7.24	1.05	0.010	-	-	0.71199
EPbg10_2	OR1	"	"	10	"	11.5	1.97	0.024	-0.250	-1.09	0.71211
EPbg3	"	"	"	3	"	7.141	0.628	0.014	-0.329	-	0.71196
EPeg10		"	einkorn	10	"	10.3	0.1	0.0	- 0.244	- 1.20	0.71173

EPmwg10		"	bread wheat	10	"	6.64	430.691	290.011	-0.351		-1.04	0.71171	
EPsg10		"	spelt	10	"	4.59	0.300	0.007	-0.376		-0.93	0.71178	
EPemg10		"	emmer	10	"	9.65	0.886	0.005	-0.317		-1.44	0.71180	
HIER2bg10_1	ORa	HIER2	hulled barley	10	"	11.8	2.10	0.023	-0.273		-0.82	0.70814	
HIER2bg10_2	ORb	"	"	10	"	8.41	1.09	0.015	-0.320	-0.353	-	0.70800	
HIER2bg3	"	"	"	3	"	9.69	0.217	0.016	-0.252		-	0.70847	
HIER2bg1	"	"	"	1	"	7.47	-	0.013	-0.298		-	0.70807	
HIER1pwg10		HIER1	rivet wheat	10	"	6.77	0.936	0.008	-0.143		-0.53	0.70833	0.70832
HIER1mwg10		"	bread wheat	10	"	13.4	0.838	0.016	-0.146		-0.22	0.70822	
GOUZmwg10		GOUZ	"	10	"	9.44	0.371	0.021	-0.222		-	0.70843	
CONVmwg10		CONV	"	10	"	16.5	1.32	0.017	-0.101		-0.61	0.70952	
EPbr		EP	hulled barley		straw	27.7	7.03	0.069	-0.182	-0.171	-	0.71215	

EPmwr	"	bread wheat	"	1.59	0.213	0.000	0.031	-	0.71057
EPemr	"	emmer	"	26.3	8.71	0.060	-0.197	-	0.71022
HIER2br	HIER2	hulled barley	"	29.7	3.78	0.091	-0.184	-	0.70810
EPbb	EP	"	awn	34.8	0.631	0.042	-0.028	-	0.71198
EPemb	"	emmer	"	19.8	3.09	0.008	-0.028	-	0.71145
HIER2bb	HIER2	hulled barley	"	60.9	2.69	0.084	0.595	-	0.70906
EPmws	EP	bread wheat	leaf	18.32	0.521	0.001	-0.168	-	0.70949
HIER2bs	HIER2	hulled barley	"	209.4	4.99	0.276	0.510	-	0.70973
CONVmwg	CONV	bread wheat	glumes	33.3	4.61	0.001	0.086	-	0.71200
EPemg10	EP	emmer	"	16.0	1.97	0.011	-0.118	-	0.71228
AL1	NIST SRM 1515	apple leaves	acid attack	311.33	0.929	0.282	0.235	-	0.71396
AL2	"	"	"	334.9	1.20	0.296	0.264	-	0.71396
Alcalc	"	"	calcinated	36	2.85	0.2	0.233	-	0.71401

	4. 4	
	4 1	

Supplementary material

A. Evolution of soil water pH between September 2018 and December 2020 inside and outside the EP. Three different depth intervals were sampled: (a) 0-10 cm; (b) 20-30 cm, and (c) 45-55 cm. In September 2018, an ash amendment was applied (pH = 9.5) inside the EP (cleared soil) while no amendment was received outside the EP.

Declaration of Competing Interest

☒ The authors declare that they have no known competing financial interests or personal relationships that could have appeared to influence the work reported in this paper.

☐The authors declare the following financial interests/personal relationships which may be considered as potential competing interests:

Highlights

- we identified which technique (marling or plant ash) was used to amend cereal crops
- $\delta^{44/40}$Ca-$\delta^{88/86}$Sr-^{87}Sr/^{86}Sr combined approach is useful for archaeological samples
- Ca and Sr have similar sources and have undergone similar fractionation mechanisms
- $\delta^{88/86}$Sr variations in grains point to biological fractionation plus source variation